

# Berry Flux Diagonalization: Application to Electric Polarization

John Bonini, David Vanderbilt, and Karin M. Rabe<sup>1</sup>

<sup>1</sup>*Department of Physics and Astronomy, Rutgers University, Piscataway, NJ 08854-8019*

(Dated: February 19, 2024)

The switching polarization of a ferroelectric is determined by the current that flows as the system is switched between two variants. Computation of the switching polarization in crystal systems has been enabled by the modern theory of polarization, where it is expressed in terms of a change in Berry phase from the initial state to the final state. It is straightforward to compute this change of phase modulo  $2\pi$ , then requiring a branch choice to specify the predicted switching polarization. The measured switching polarization depends on the actual path along which the system is switched, which in general involves nucleation and growth of domains and is therefore quite complex. In this work we present a first principles approach for predicting the switching polarization that requires only a knowledge of the initial and final states, based on the empirical observation that for most ferroelectrics, the observed polarization change is the same as for a path involving minimal evolution of the state. To compute the change along a generic minimal path, we decompose the change of Berry phase into many small contributions, each much less than  $2\pi$ , allowing for a natural resolution of the branch choice. We show that for typical ferroelectrics, including those that would have otherwise required a densely sampled path, this technique allows the switching polarization to be computed without any need for intermediate sampling between oppositely polarized states.

## I. INTRODUCTION

Bistable systems with a change in electric polarization on switching between the two states are of central importance in functional material and device design. The most familiar of such systems are ferroelectrics, with two or more symmetry-related polar insulating states.<sup>1</sup> Switching in systems in which the two states are not symmetry related, for example in antiferroelectrics or heterostructures, is also of great interest for novel devices.<sup>2,3</sup>

First principles prediction of the switching polarization in periodic systems is based on the modern theory of polarization, which expresses the polarization change between two states in terms of the change in Berry phase as the system evolves along a specified adiabatic path.<sup>4,5</sup> From knowledge of the initial and final states, the polarization change is determined modulo the “quantum of polarization” ( $e\mathbf{R}/\Omega$ ), where  $e$  is the charge of an electron,  $\mathbf{R}$  is a lattice vector, and  $\Omega$  is the volume of the unit cell. Additional information about the path would be needed to determine which of the allowed values corresponds to any given path.

Since the path for a process such as electric field switching of a ferroelectric generally involves nucleation and growth of domains, beyond the scope of current first-principles computation, it might at first seem that first-principles prediction of the switching polarization should not be possible. However, it is an empirical fact that good agreement with experimental observation has been obtained for many ferroelectrics by computing the polarization change along a fictitious minimal path,<sup>6–8</sup> usually constructed by simple linear interpolation of the atomic positions of the up- and down-polarized states, maintaining their lattice translational symmetries. The polarization change along this fictitious path is then computed by sampling densely enough along the path so that the polarization change for every step along the path can

be chosen (and is chosen) to be small compared to the quantum of polarization. However, this method can be computationally intensive, depending on the sampling density required. Moreover, for some systems, it might be that not all the states on the simple linear interpolation path are insulating, and additional effort is required to find an insulating adiabatic path connecting the up and down states. As a result, this approach has proven to be problematic for automated high-throughput applications.<sup>9</sup>

In this paper, we present a new method for predicting switching polarization given only the initial and final states. Our approach uses information, computed from the two sets of ground state wavefunctions, that goes beyond that used in a conventional Berry phase calculation. The key idea is to incorporate certain assumptions about the physical path, eliminating the need to construct a fictitious path and perform calculations for intermediate states. We begin by discussing the method for the simplest case of the electronic contribution to the switching polarization for a one-dimensional polar insulator. We then generalize to three-dimensional materials and discuss the ionic contribution to the polarization. Finally, first-principles results are presented for a realistic benchmark system to illustrate the various aspects of the method and to compare with the fictitious path method. The approach presented here is not limited to computation of switching polarization in ferroelectrics, but can be applied to the change in polarization between two symmetry-inequivalent states, for example in antiferroelectrics, heterostructures and pyroelectrics, and in the computation of the nonlinear response of insulators to electric fields.

## II. FORMALISM

### A. Background and notation

We start by considering a one-dimensional crystal switching from initial state  $A$  to final state  $B$  along a specified path, parameterized by  $\lambda$ , along which the system remains insulating. According to the modern theory of polarization,<sup>4,5,8,10</sup> the electronic contribution to the change in polarization can be expressed as

$$\Delta P_{A \rightarrow B} = \frac{-e}{2\pi} \Phi \quad (1)$$

where  $\Phi$  is the Berry flux

$$\Phi = \int \int_S \Omega(k, \lambda) d\lambda dk \quad (2)$$

obtained by integrating the Berry curvature  $\Omega(k, \lambda)$  over the region  $S$  with  $\lambda_A \leq \lambda \leq \lambda_B$  and  $-\pi/a < k \leq \pi/a$  (the first Brillouin zone). Here the Berry curvature

$$\Omega(k, \lambda) = \sum_n -2\text{Im} \langle \partial_\lambda u_n(k, \lambda) | \partial_k u_n(k, \lambda) \rangle \quad (3)$$

is written in terms of the cell-periodic parts of the occupied Bloch wavefunctions  $|u_n(k, \lambda)\rangle$  and has been traced over the occupied bands  $n$ . The existence of the derivatives in Eq. (3) requires choice of a ‘‘smooth gauge’’: that is, for a single occupied band, the  $k$ - and  $\lambda$ -dependent phase of the wave functions  $|u(k, \lambda)\rangle$  must be chosen so that  $|u(k, \lambda)\rangle$  is differentiable as a function of  $k$  and  $\lambda$  over all of  $S$ . For multiple occupied bands, specification of a gauge may involve a  $(k, \lambda)$ -dependent unitary rotation of the occupied bands. Since physical observables like the change in polarization along a specified path do not depend on the choice of gauge, we are free to choose a gauge for which the  $|u_n(k, \lambda)\rangle$  are periodic in  $k$ .

Application of Stoke’s theorem gives

$$\Phi = \oint_C \mathbf{A}(\mathbf{q}) \cdot d\mathbf{q} \quad (4)$$

where  $C$  is the boundary of the surface  $S$ ,  $\mathbf{q} = (k, \lambda)$ , and  $\mathbf{A}(\mathbf{q}) = (A_k, A_\lambda)$  is the Berry potential given by

$$A_k = \sum_n i \langle u_n(k, \lambda) | \partial_k u_n(k, \lambda) \rangle, \quad (5)$$

$$A_\lambda = \sum_n i \langle u_n(k, \lambda) | \partial_\lambda u_n(k, \lambda) \rangle. \quad (6)$$

Since we have chosen a gauge periodic in  $k$ , we have  $|u_n(k + 2\pi, \lambda)\rangle = |u_n(k, \lambda)\rangle$ . Then, we have  $A_\lambda(k + 2\pi, \lambda) = A_\lambda(k, \lambda)$  and the contributions  $\int_0^1 A_\lambda(k, \lambda) d\lambda$  and  $\int_1^0 A_\lambda(k + 2\pi, \lambda) d\lambda$  from the two portions of the path  $C$  along the  $\lambda$  direction cancel. The two remaining segments take the form

$$\phi_\lambda = \int_{-\pi/a}^{\pi/a} A_k(k, \lambda) dk \quad (7)$$

and it follows that

$$\Phi = \phi_{\lambda_B} - \phi_{\lambda_A}. \quad (8)$$

The electronic contribution to the change in polarization is then given by Eq. (1).

While the evaluation of 8 requires only wavefunctions on the boundary of  $S$ , the equivalence of Eqs. (2) and (8) requires the existence of a smooth gauge on all of  $S$  that matches the choice of gauge on the boundary. If the gauge is required to be smooth only on the boundary of  $S$ , without this additional constraint, then a gauge transformation can change quantities such as  $\phi_{\lambda_A}$  and  $\phi_{\lambda_B}$  by multiples of  $2\pi$ .<sup>4,5,8</sup> We refer to such quantities as ‘‘gauge invariant modulo a quantum,’’ in distinction to quantities which are ‘‘fully gauge invariant,’’ and to ‘‘fully gauge dependent’’ quantities that can take on any value in a continuous range with a change in gauge. In this case  $\Phi$  in Eq. (8) is determined only modulo  $2\pi$ , and the change in polarization is determined only modulo the quantum of polarization  $e\mathbf{R}/\Omega$ .

In other words, Eq. (2) is the fundamental expression for the change in polarization along a specified path. It depends on the wavefunctions at all intermediate  $k$  and  $\lambda$  and is fully invariant under gauge transformation of the wavefunctions. On the other hand, the Berry phase difference Eq. (8) depends only on the wavefunctions on two edges of the boundary of  $S$ , and under gauge transformation of these wavefunctions is only gauge invariant modulo a quantum. It is equal to the change in polarization along the specified path only if the gauge chosen on the boundary is one that can be smoothly continued into the interior onto the wavefunctions at all intermediate  $k$  and  $\lambda$ .

The fictitious minimal path method, the most widely used method for resolving the branch choice for the difference  $\phi_{\lambda_B} - \phi_{\lambda_A}$  to compute the change in polarization along a specified path, relies on sampling a minimal path, usually obtained by linear interpolation, at intermediate values of  $\lambda$ . The density of sampling increased until each new  $\phi_{\lambda_{j+1}}$  can be chosen such that  $|\phi_{\lambda_{j+1}} - \phi_{\lambda_j}| \ll \pi$ . With a sufficiently dense sampling the branch choice identified by this procedure will match that of the continuum formulation, giving the correct polarization change for this path. In practice the computation of  $\phi_\lambda$  requires a discretization in  $k$ . Sec. II C provides more details on how the relevant quantities are computed when states are sampled on a discrete mesh.

Here, we present an alternative approach to resolving the branch choice that makes full use of the information contained in the initial and final states, while eliminating the need for sampling at intermediate values of  $\lambda$ . Moreover, this approach requires a  $k$ -space sampling no denser than that required for the computation of the formal polarization. Like the previous methods, the fully gauge-invariant quantity  $\Phi$  is separated in to smaller contributions that, while gauge-invariant only modulo  $2\pi$  in principle, can always be taken much smaller than  $2\pi$  in practice. However, here the construction relies only on

the wavefunctions of the initial and final states, without reference to intermediate steps along the path. The additional assumption required for this procedure is that the initial and final states at  $\lambda_A$  and  $\lambda_B$  must be similar enough that their gauges can be aligned, in a sense to be described shortly. Essentially, the gauge alignment procedure implements a minimal evolution of the electronic structure, in analogy with the previously assumed minimal evolution of the ionic structure.

### B. Gauge class

We first consider the case of a single occupied band in 1D with Bloch states  $|u(k)\rangle$ . Following Eq. (8), the Berry phase around the Brillouin zone at a given  $\lambda$  is given by

$$\phi = \int_{-\pi/a}^{\pi/a} \langle u(k) | i\partial_k u(k) \rangle dk \quad (9)$$

and, following the terminology introduced in the previous section, is gauge invariant modulo a quantum: specification of a gauge that is smooth on the first Brillouin zone and periodic in  $k$  allows transformations of the form  $e^{-i\beta(k)} |u(k)\rangle$ , where  $\beta(k)$  is differentiable and  $\beta(k + 2\pi/a) = \beta(k) + 2\pi n$  for some integer  $n$ , which changes  $\phi$  by  $2\pi n$ . For a given physical system, we can test whether two choices of gauge  $a$  and  $b$  will produce the same value of  $\phi$  by computing

$$\gamma^{ab}(k) = \langle u^a(k) | u^b(k) \rangle. \quad (10)$$

Note that  $\gamma^{ab}(k)$  has exactly unit norm and is just  $e^{-i\beta(k)}$ , where  $\beta(k)$  describes the gauge change relating  $a$  to  $b$ . If  $\gamma^{ab}(k)$  is smooth and its phase does not wind by a nonzero integer multiple of  $2\pi$  as  $k$  traverses the 1D Brillouin zone, the two gauges will produce the same  $\phi$ , and can be said to belong to the same ‘‘gauge class.’’

Next, we consider two crystals  $A$  and  $B$  with single occupied bands, each with a smooth gauge, and ask whether their respective gauges belong to the same gauge class in a similar sense. With this motivation, we define, in analogy with Eq. (10),

$$\gamma^{AB}(k) = \langle u^A(k) | u^B(k) \rangle \quad (11)$$

where  $\gamma^{AB}(k)$  will generally not have unit norm. In fact, for this procedure to be meaningful, systems  $A$  and  $B$  must be sufficiently closely related that the norm of  $\gamma^{AB}(k)$  remains nonzero everywhere in the Brillouin zone. If the phase of this  $\gamma^{AB}(k)$  does not wind by a nonzero integer multiple of  $2\pi$ , we consider their gauges to belong to the same gauge class.

We are now in a position to introduce our key idea for the prediction of the switching polarization from system  $A$  to  $B$ . We recall the empirical fact, discussed in the Introduction, that good agreement with experimental observation has been obtained for many ferroelectrics by computing the polarization change along a fictitious

minimal path. Our insight is that in general, along such paths, the wavefunction phases will evolve in a minimal way that preserves the gauge class, so that the switching polarization corresponds to the polarization difference of Eq. (1) and Eq. (8) with Berry phases  $\phi^A$  and  $\phi^B$  computed with the requirement that the two gauges belong to the same gauge class. Crucially, the branch-choice ambiguity in the individual  $\phi^A$  and  $\phi^B$  is no longer present after the difference is taken.

The generalization to the multiband case is straightforward. We define

$$\gamma^{AB}(k) = \det M^{AB}(k) \quad (12)$$

where  $M^{AB}(k)$  is the overlap matrix given by

$$M_{mn}^{AB}(k) = \langle u_m^A(k) | u_n^B(k) \rangle \quad (13)$$

for occupied band indices  $m$  and  $n$ . The gauges are said to belong to the same class if the phase winding of  $\gamma^{AB}(k)$  is zero.

One way to insure that gauges  $A$  and  $B$  belong to the same gauge class is to align one to the other. In the single-band case, the gauge of  $B$  is aligned to that of  $A$  by taking  $\chi(k) = \text{Im} \ln \gamma^{AB}(k)$ , and then letting

$$|\tilde{u}^B(k)\rangle = e^{-i\chi(k)} |u^B(k)\rangle. \quad (14)$$

As a result, the new  $\tilde{\gamma}^{AB}(k)$  is real and positive, so that there is clearly no winding. Similarly, the multiband gauge alignment can be accomplished by carrying out the singular value decomposition of  $M^{AB}$  in Eq. (12) as  $M^{AB} = V^\dagger \Sigma W$ , where  $V$  and  $W$  are unitary and  $\Sigma$  is positive real diagonal. Then the multiband analog of  $e^{i\chi}$  is  $U = V^\dagger W$ , and the gauge of  $B$  is aligned to that of  $A$  by the transformation

$$|\tilde{u}_n^B\rangle = \sum_m (U^\dagger)_{mn} |u_m^B\rangle. \quad (15)$$

The new overlap matrix is then  $\tilde{M}^{AB} = V^\dagger \Sigma V$ , whose determinant  $\tilde{\gamma}^{AB}$  in Eq. (12) is clearly real and positive, thus eliminating the relative winding of gauge  $B$  with respect to  $A$ .

The physical interpretation of enforcing both systems to belong to the same gauge class is that we are assuming a minimal evolution of the electronic states. If the initial and final states represent exactly the same bulk system, the result of this procedure is obviously that the change in polarization is zero. In this situation, other choices of gauge that give a nonzero value describe a physical path where one or more quanta of charge are pumped by a lattice vector over an adiabatic cycle with the periodic system returning to its initial state. In making the same-gauge-class assumption for systems where the initial and final states are different, but still closely related, we similarly identify a result which involves a minimal evolution of the state. An analogy can be made with the implicit assumptions already being made when one constructs a switching path for the ions. When comparing

initial and final states, one typically specifies which ion maps to which by minimizing displacements between ions of the same species, e.g., such that no ion moves by more than half a unit cell. The gauge alignment procedure described above does something similar, mapping which band goes with which by maximizing wavefunction overlaps and eliminating phase differences at corresponding  $k$ -points.

### C. Discrete $k$ space

In any numerical calculation, functions of  $k$  must be sampled on a discrete mesh in  $k$ . In this case, we can again align the gauge of  $B$  to that of  $A$  using Eq. (14) or Eq. (15), and compute the polarization difference via Eq. (8). However, in the discrete case there is a new potential source of ambiguity coming from the need to enforce smoothness with respect to  $k$ . After discretization Eq. (7) becomes

$$\phi_\lambda = \text{Im} \ln \det \prod_i M^\lambda(k_i, k_{i+1}) \quad (16)$$

where  $M$  is the overlap matrix

$$M_{mn}^\lambda(k_i, k_{i+1}) = \langle u_m^\lambda(k_i) | u_n^\lambda(k_{i+1}) \rangle. \quad (17)$$

This  $\phi_\lambda$  is gauge-invariant, but only up to an integer multiple of  $2\pi$ . This is reflected by the  $\text{Im} \ln$  operation in Eq. (16), which will only result in a phase in the interval  $-\pi < \phi_\lambda < \pi$ . If one is interested in this phase on its own (i.e., for computing formal polarization) this makes perfect sense, since it is truly a lattice valued quantity. However, our present goal is to compute the difference in phase between two systems with the requirement that both systems are in the same gauge class. For this purpose it is useful to rewrite Eq. (16) in a form where values outside this interval are possible (with the branch being determined by the gauge). To this end we rewrite Eq. (16) as

$$\phi_\lambda = \sum_i \mathcal{A}_i(\lambda) \quad (18)$$

where

$$\mathcal{A}_i(\lambda) = \text{Im} \ln \det M_\lambda(k_i, k_{i+1}) \quad (19)$$

is a discrete analog of the Berry connection  $A_k$ . We choose a sufficiently fine  $k$  mesh and a sufficiently smooth gauge so that each  $\mathcal{A}_i$  is much less than  $\pi$  in magnitude; then  $\phi^A$  can be unambiguously computed (for the chosen gauge). We then choose the gauge in  $B$  to be aligned to that of  $A$ . Assuming this also results in a smooth gauge in  $B$ , we could then confidently compute  $\Delta P$  from Eqs. (1) and Eq. (8).

### D. Gauge invariant formulation

The procedure described in the last section involved constructing a smooth gauge in  $A$ , aligning the gauge in  $B$ , and then computing each  $\phi_\lambda$  via Eq. (18). This represents a straightforward, but also inconvenient, means of applying the same gauge class assumption to a realistic calculation. In this section and the next we will develop an equivalent procedure that is more computationally efficient and does not require explicit construction of smooth or aligned gauges.

First, we note that the value obtained above is equivalent to evaluating  $\Phi$  as

$$\Phi = \sum_i \Delta \mathcal{A}_i \quad (20)$$

where

$$\Delta \mathcal{A}_i = \mathcal{A}_i(\lambda_B) - \mathcal{A}_i(\lambda_A) \quad (21)$$

is the difference between Eq. (19) evaluated at the initial and final configurations (with the previously discussed gauge choices). At present, it is required that  $k$  has been sampled densely enough such that each  $\Delta \mathcal{A}_i$  is smaller in magnitude than  $\pi$ .

We next note that the quantity  $\Delta \mathcal{A}_i$  is equal to the discrete Berry phase computed around the perimeter of the rectangular plaquette marked by the green arrows in Fig. (1). To see this, we denote the four corners of this plaquette as  $\mathbf{q}_1 = (k_i, \lambda_A)$ ,  $\mathbf{q}_2 = (k_i, \lambda_B)$ ,  $\mathbf{q}_3 = (k_{i+1}, \lambda_B)$ , and  $\mathbf{q}_4 = (k_{i+1}, \lambda_A)$ , and refer to it henceforth as plaquette  $p$  located at  $k_i = k_p$ . Defining the overlap matrices

$$M_{mn}^{(ij)} = \langle u_m(\mathbf{q}_i) | u_n(\mathbf{q}_j) \rangle, \quad (22)$$

the four-point Berry phase about the loop, traced over occupied bands, is

$$\phi^p = \text{Im} \ln \det [M^{(12)} M^{(23)} M^{(34)} M^{(41)}]. \quad (23)$$

This four-point Berry phase is equal to the Berry flux through the plaquette, by the same Stoke's theorem argument used to relate Eq. (2) and Eq. (4). This plaquette Berry flux,  $\phi_i$ , can be seen to be equal to  $\Delta \mathcal{A}_i$  computed with the gauges specified above since the alignment of gauges insures that  $M^{(12)}$  and  $M^{(34)}$  have real positive determinants, and thus don't contribute to the phase being extracted by the  $\text{Im} \ln$  operation. The advantage of computing  $\phi^p$  as in Eq. (23) is that it is completely insensitive to the gauges used to represent the states at any of the four  $\mathbf{q}_i$ .<sup>11</sup> Using Eq. (20) we can write  $\Phi$  as the sum over plaquette Berry fluxes,

$$\Phi = \sum_p \phi^p. \quad (24)$$

As the  $\text{Im} \ln$  operation suggests,  $\phi^p$  is only gauge invariant up to an integer multiple of  $2\pi$ , so the above formula still requires that the  $k$ -mesh spacing be fine enough that each  $|\phi^p| < \pi$  for all  $k_p$ , just as was required for  $\Delta \mathcal{A}_i$ .

### E. Berry flux diagonalization

With Eqs. (1), (23) and (24), one can compute the polarization difference using arbitrarily chosen gauges for systems  $A$  and  $B$ . However, there is still a requirement that the  $k$ -mesh be fine enough that all  $\phi_p$  in Eq. (24) are smaller in magnitude than  $\pi$ . For a single-band system, this typically does not require a mesh any finer than that needed to compute  $\phi_\lambda$  from Eq. (16). However, the plaquette Berry fluxes  $\phi^p$  from Eq. (23) are traced over all occupied bands, so their values can quickly grow much larger in magnitude than  $\pi$  when many bands are contributing.

We can instead decompose each plaquette flux into a sum  $\phi_p = \sum_n \phi_n^p$  of smaller gauge-invariant phases  $\phi_n^p$ , where  $n$  runs over the number of occupied bands. These are the multi-band Berry phases or Wilson loop eigenvalues of plaquette  $p$ , obtained from the unitary evolution matrix  $\mathfrak{U}_p$  acquired by traversing the boundary of the plaquette. Explicitly,

$$\mathfrak{U}_p = \mathcal{M}^{(12)} \mathcal{M}^{(23)} \mathcal{M}^{(34)} \mathcal{M}^{(41)} \quad (25)$$

where  $\mathcal{M}^{(ij)}$  is the unitary approximant of  $M^{(ij)}$ , that is,  $\mathcal{M} = V^\dagger W$  where

$$M = V^\dagger \Sigma W \quad (26)$$

is the singular value decomposition of  $M$ . The eigenvalues of the unitary matrix  $\mathfrak{U}_p$  are of the form  $e^{i\phi_n^p}$ , providing the needed  $\phi_n^p$ , which are gauge-invariant. Since  $\text{Im} \ln \det \mathfrak{U}_p$  is taken as the Berry flux through plaquette  $p$ , we have in a sense diagonalized this Berry flux by obtaining the eigenvalues of  $\mathfrak{U}_p$ . Finally, the  $\phi_n^p$  can be summed over all plaquettes to obtain the total polarization difference via

$$\Phi = \sum_p \sum_n \phi_n^p. \quad (27)$$

This is our central result.

For the method to be applicable the two states  $\lambda_A$  and  $\lambda_B$  must be similar enough that the singular values in  $\Sigma$  do not become too small (this corresponds to the continuum-case requirement that the norm of  $\gamma^{AB}$  in Eq. (11) should remain nonzero). For agreement with the continuum case the individual  $\phi_n^p$  must each be much smaller in magnitude than  $\pi$ . This condition is typically satisfied with a  $k$ -mesh density appropriate for a standard Berry-phase polarization calculation, but the density of the  $k$  mesh could be increased if necessary. These conditions are further discussed in Section V C.

The above expressions were all written for the one-dimensional case for the sake of simplicity; the generalization to two and three dimensions is quite straightforward. Just as is typically done for the computation of the Berry-phase polarization, the computation is carried out separately for each string of  $k$ -points in the direction of the desired polarization component, and the results are then averaged over the complementary directions.

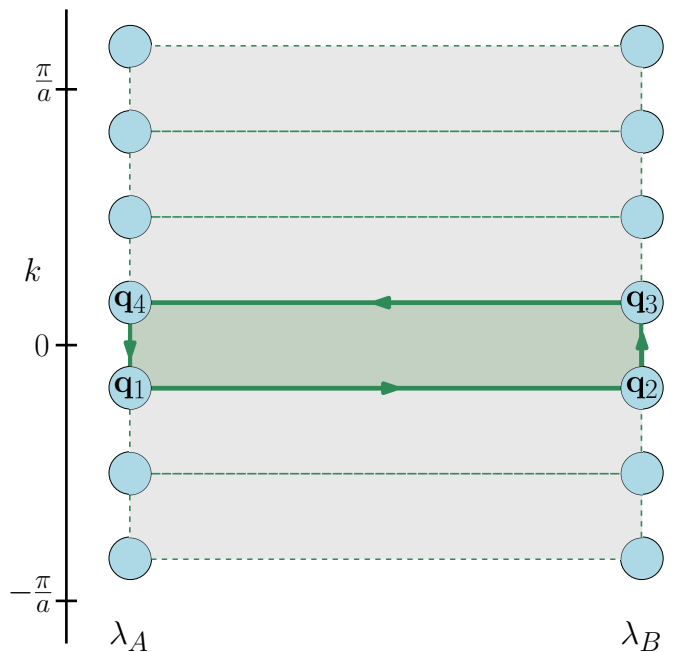


FIG. 1. Sketch of the joint  $(k, \lambda)$  space for computing a change in polarization between  $\lambda_A$  and  $\lambda_B$ . Blue circles represent points where Bloch wavefunctions have been computed. The light grey box represents the surface  $S$  that is integrated over in Eq. (2). Dotted green lines represent the plaquettes  $i$  and the solid green lines represent the path on which the parallel transport procedure is performed around the green plaquette it encloses to obtain its contribution to  $P^B - P^A$ .

Note that while the computation of overlap matrices between neighboring  $k$ -points is quite routine, this procedure also requires overlaps between wavefunctions of corresponding  $k$ -points at different  $\lambda$  values (typically different structures). The implementation details for this procedure are discussed in Sec. III.

### F. Ionic contribution and alignment

Up to this point, we have focused only on computing the electronic contribution to the change in polarization for already fixed choices of unit cells at each  $\lambda$ . Differences in origin choice and cell orientation between  $\lambda_A$  and  $\lambda_B$  in general will change the decomposition of the Berry phase polarization into electronic and ionic contributions, and in particular can alter the Bloch function overlaps in Eq. (17).<sup>12</sup> The Berry flux diagonalization method is most robust when structures are aligned to maximize overlaps, and thus keep elements of the  $\Sigma$  matrix in Eq. (26) (the singular values) from becoming too small. We make this choice of unit cell by first aligning the structures to minimize the root mean squared displacements of the ionic coordinates. After this initial alignment, we further refine the choice of origin by translating along the polarization direction to maximize the smallest of all the singular values encountered while

scanning over all  $k$ -points in the above-described procedure. This additional refinement can be performed without additional first-principles calculations using the existing wavefunctions; in the plane-wave representation this is accomplished by computing

$$M_{mn}^{(AB)}(\mathbf{k}) = \langle \psi_{m\mathbf{k}}^A | T_\tau \psi_{n\mathbf{k}}^B \rangle = \sum_{\mathbf{G}} C_{m,\mathbf{G}+\mathbf{k}}^{(A)*} C_{n,\mathbf{G}+\mathbf{k}}^{(B)} e^{-i\mathbf{G}\cdot\tau}$$

where  $T_\tau$  is the extra translation by  $\tau$  and the  $C_{n,\mathbf{G}+\mathbf{k}}$  are the plane wave coefficients.

The ionic contribution to the polarization change is given by

$$\Delta \mathbf{P}_{\text{ion}} = \frac{e}{V_{\text{cell}}} \sum_i Z_i \Delta \mathbf{r}_i \quad (28)$$

where  $\Delta \mathbf{r}_i$  is the displacement of ion  $i$  between states  $\lambda_A$  and  $\lambda_B$ .

### III. METHODS

The Berry flux diagonalization method is a post-processing step for wavefunctions generated by first-principles density-functional-theory codes. Our current implementation of the method<sup>13</sup> is for wavefunctions in a plane-wave basis. Here we perform calculations in ABINIT using the norm conserving scalar relativistic ONCVSP v0.3 pseudopotentials with the LDA exchange correlation functional.<sup>14</sup> The necessary overlap matrices are computed from the NetCDF wavefunction files produced by ABINIT, read using the abipy library<sup>15</sup> (<https://github.com/abinit/abipy>). The pymatgen library<sup>16</sup> is used in the process of computing the ionic contribution.

We validate and demonstrate the Berry flux diagonalization method as follows. First, we use the method to compute the switching polarization of the prototypical ferroelectric perovskite oxides BaTiO<sub>3</sub>, KNbO<sub>3</sub>, and PbTiO<sub>3</sub>, for which the computation of the switching polarization by existing methods is straightforward. We then compute the switching polarization of pure PbTiO<sub>3</sub> and PbTi<sub>0.75</sub>Zr<sub>0.25</sub>O<sub>3</sub> with a  $2 \times 2 \times 1$  supercell, using both the present method and the fictitious minimal path method for direct comparison. The atomic positions in PbTi<sub>0.75</sub>Zr<sub>0.25</sub>O<sub>3</sub> were taken to be the same as in the pure system.

### IV. RESULTS

The computed switching polarizations for the prototypical ferroelectric perovskite oxides BaTiO<sub>3</sub>, KNbO<sub>3</sub>, and PbTiO<sub>3</sub>, are 0.26 C/m<sup>2</sup>, 0.29 C/m<sup>2</sup>, and 0.77 C/m<sup>2</sup> respectively, resolving the branch choice in the Berry phase differences with the quantum of polarization for the primitive cells being 1.04 C/m<sup>2</sup>, 1.03 C/m<sup>2</sup>, and 1.08 C/m<sup>2</sup>, respectively. These switching polarization values

are in complete agreement with reported first-principles values obtained by the fictitious minimal path approach, which have previously been established to be in good agreement with experimental observations.<sup>6</sup> In this section, we give a detailed analysis of the results for pure PbTiO<sub>3</sub>, which has the largest polarization and thus presents the most difficulties of the three. We do this for three cases, namely in the primitive 5-atom cell, in a  $2 \times 2 \times 1$  supercell, and in the same supercell, but with one Ti replaced by Zr.

The key quantities here are the Wilson loop eigenvalues, which are summed in Eq. (27) to obtain the change in polarization. For PbTiO<sub>3</sub>, the distribution of the Wilson loop eigenvalues is shown in Fig. 2 for plaquettes along the string of  $k$ -points corresponding to  $k_x = \pi/4a, k_y = \pi/4a$  for the primitive cells, and to the corresponding point  $k_x = \pi/2a, k_y = \pi/2a$  for the supercell systems. All Wilson loop eigenvalues are found to be much smaller in magnitude than  $\pi$ , mostly clustered around zero, with a bias in the direction of the electronic polarization change. Here this is negative given the choice of initial and final states.

Each individual contribution to the change in polarization for the supercell is identical to that of the primitive cell, except that they appear with multiplicity four due to the translational symmetries that were lost in the supercell system. So, while the change in dipole moment for the supercell is four times as large as that for the primitive unit cell, and is thus significantly larger than the  $2\pi$  phase ambiguity, this does not present any difficulties in the Berry flux method.

The Wilson loop eigenvalues for the system with one Ti replaced by Zr is shown in the left portion of Fig. 2. All eigenvalues fall in the same range as the pure PbTiO<sub>3</sub> system, but with some splitting of values. The switching polarization for the system with Zr was found to be 0.762 C/m<sup>2</sup> compared to the slightly larger 0.771 C/m<sup>2</sup> of the pure system.

In Fig. 3, we show the singular values of overlap matrices  $M$  between initial and final states at corresponding  $k$ -points for PbTiO<sub>3</sub> in its primitive cell. These singular values are the diagonal elements of  $\Sigma$  from Eq. (26). If the singular values do not approach zero at any point in the Brillouin zone, the computed information for initial and final states determines the polarization change within the same gauge class assumption. Fig. 3 shows that the singular values for PbTiO<sub>3</sub> are well behaved.

### V. DISCUSSION

#### A. Comparison to fictitious path approach

In this section we compare the Berry flux diagonalization method to the commonly used fictitious path approach,<sup>7,17,18</sup> using PbTiO<sub>3</sub> in its primitive cell and in a  $2 \times 2 \times 1$  supercell as illustration.

For the fictitious path approach, we choose a simple

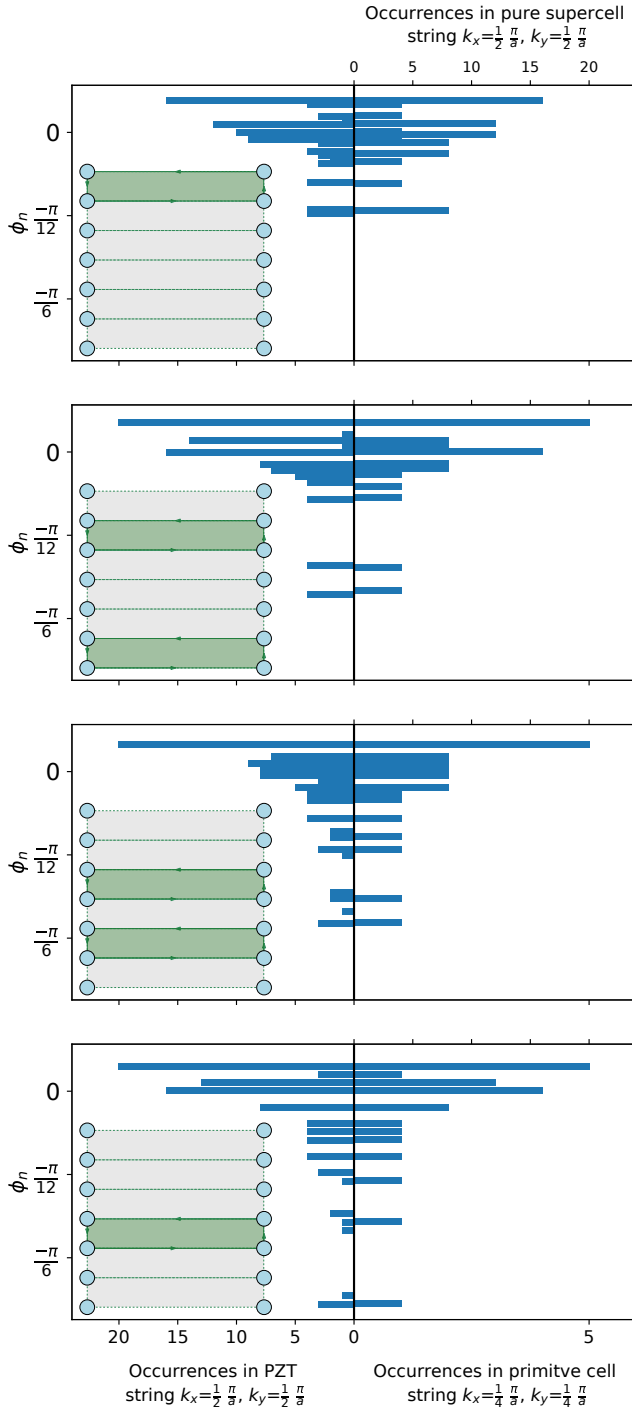


FIG. 2. Histogram of Wilson loop eigenvalues ( $\phi_n^p$  from Eq. (27)) for the plaquettes highlighted in the insets following the form of Fig. 1. In each of the two middle plots, the two highlighted plaquettes have identical contributions due to time reversal symmetry. Values for pure  $\text{PbTiO}_3$  are shown on the right. The occurrences of values for the primitive and supercell systems differ only by a factor of 4 as indicated by the two axis scales at the top and bottom of the figure. Values for  $\text{PbZr}_{0.25}\text{Ti}_{0.75}\text{O}_3$  are shown at left.

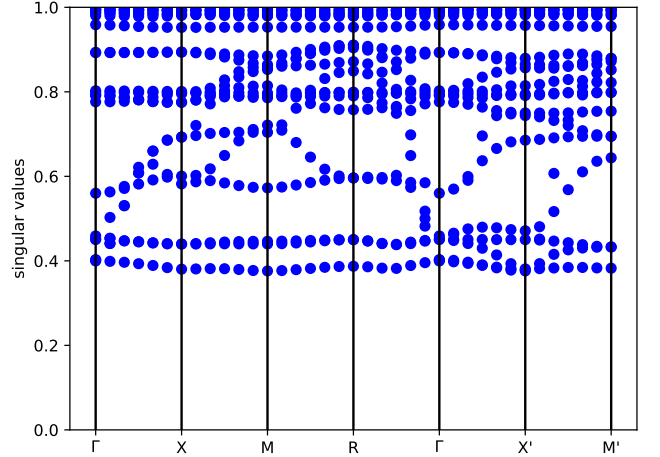


FIG. 3. Singular values throughout the Brillouin zone for  $\text{PbTiO}_3$ , sampled on a  $12 \times 12 \times 12$   $\Gamma$  centered  $k$  mesh.

linearly interpolated path between oppositely polarized states. Fig. 4 shows the formal polarization which is determined modulo the polarization quantum, computed at points along the path for two different sampling densities. Starting with an arbitrary choice for the initial state, the branch is chosen by connecting to the closest value for the next sampled state along the path. The difference between the final and initial states is then divided by two to get the spontaneous polarization.

For the case of the primitive cell, calculations for three intermediate states on the path are needed correctly to resolve the branch ambiguity. In the case of the supercell, because of the four-fold decrease in the polarization quantum, the number is significantly larger: 15 intermediate calculations must be done to resolve the branch ambiguity. The Berry flux diagonalization approach in both cases, shown by the blue arrow, predicts the change in polarization (with the correct branch choice) using only the wavefunctions in the initial and final states.

We note that other approaches have been discussed that utilize partial information in addition the evolution of  $P_{\text{formal}}$ , such as nominal valence charges and Born effective charges.<sup>5</sup> This additional information can help determine the choice of polarization value at the next point on the path even when this is not the smallest change, reducing the sampling density needed. However, the implementation tends to be ad-hoc and is not suitable for automated high-throughput applications. Furthermore, such approaches may not be reliable in situations where these assumed charges are not constant through the switching process.

## B. Relation to Wannier functions

The Wilson loop eigenvalues  $\phi_n^p$  used in Eq. (27) and shown in Fig. 2 have a close relation to the position expectation value of maximally localized Wannier func-

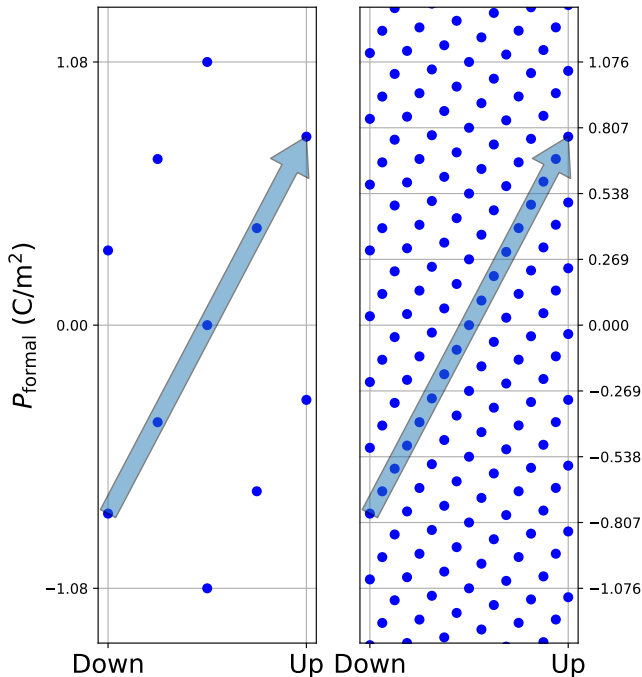


FIG. 4. Evolution of formal polarization of  $\text{PbTiO}_3$  along a linearly interpolated switching path for the primitive cell (left) and a  $2 \times 2 \times 1$  supercell (right). Ticks and horizontal lines mark the polarization quantum. The blue arrow indicates the change in polarization, which with the Berry flux diagonalization method only requires calculations in the initial state and symmetry-related final state.

tions, which we refer to maximally localized Wannier centers.<sup>19</sup> The parallel transport procedure used in obtaining these  $\phi_n^p$  is precisely the same as that used in obtaining the Wannier centers maximally localized along one dimension. In the Berry flux diagonalization method the procedure is performed around the plaquettes, while when computing maximally localized Wannier functions the procedure is performed across the loop formed by traversing the Brillouin zone at a single  $\lambda$ . In the Wannier case, the Wilson loop eigenvalues obtained are complex numbers with phase  $2\pi r_n/a$ , with the  $r_n$  being the maximally localized Wannier centers.<sup>20</sup> The  $r_n$  can be treated as the positions of point charges to compute the formal polarization.<sup>20</sup> Similarly, the Wilson loop eigenvalues obtained in the Berry flux diagonalization method can be understood as contributions to changes in positions of point charges, yielding the change in formal polarization.

### C. Conditions for applicability

To make the correct branch choice and compute the change in polarization, some assumption about the dynamics of the switching process must be made. In the method presented in this work, the assumption is that the system evolves in some minimal way between oppositely

polarized states, based on the empirical fact that computation of the polarization change along a fictitious minimal path generally corresponds to the measured value. Ionic contributions to the change in polarization are separated by assuming displacements are minimized, and electronic contributions are separated by assuming that as the wavefunctions evolve along the physical switching path, they maintain a high degree of overlap.

This regime where the latter assumption breaks down can be detected automatically. When the changes in the electronic states across changes in  $\lambda$  becomes large, the overlaps in wavefunctions become small, and some singular values of the  $\Sigma$  matrix of Eq. (26) approach zero. The implementation of the method checks to make sure that no singular values anywhere in the Brillouin zone fall below a threshold (see Fig. 3). Numerical experiments have shown that a threshold of around 0.15 seems to work well for systems tested. There is of course also a branch ambiguity if the Wilson loop eigenvalues ( $\phi_n^p$  of Eq. (27)) have magnitudes close to  $\pi$ . In practice, we have found no cases where this happens without the requirement on the singular values failing first. This can be understood from the viewpoint that the Wilson loop eigenvalues are related to displacements of Wannier centers, with a value of  $\pi$  corresponding to a single charge moving by half a unit cell. When the charge is moved over such a distance the overlaps tend to become small, especially in an insulating system where states are localized. For such systems, one can revert to constructing intermediate states along  $\lambda$ . If each change in polarization is computed using the Berry flux diagonalization method,  $\lambda$  can be sampled more coarsely than methods that track only the total phase. However, in doing so one should beware of making possibly unsafe assumptions about the dynamics of the switching process.

## VI. CONCLUSION

The Berry flux diagonalization method presented here provides a way to compute the change in polarization that is more easily automated, as well less computationally expensive, than existing approaches. The magnitudes of the singular values obtained in the course of the calculation provide a built-in test of whether the two systems being compared are sufficiently similar that a class of minimal paths producing the same change in polarization can be inferred. Future work will explore the application of this method to the change in polarization between two states that are not symmetry related, such as in pyroelectrics, antiferroelectrics, heterostructures and insulators in finite electric fields. It will also be interesting to test the applicability of the approach to different classes of ferroelectrics, such as organic, inorganic order-disorder, charge-ordered, or improper ferroelectrics. Generalizations of the method to the computation of other quantities requiring Berry curvature integration, such as Chern numbers and characterization

of Weyl points, should also reward future investigation.

We would like to thank Don Hamann and Cyrus Dreyer for useful discussions.

## VII. ACKNOWLEDGMENTS

This work was supported by ONR Grant N00014-16-1-2951, ONR N00014-17-1-2770, and NSF DMR-1334428.

- 
- <sup>1</sup> M. E. Lines and A. M. Glass, “Principles and applications of ferroelectrics and related materials,” (2001), 10.1093/acprof:oso/9780198507789.001.0001.
- <sup>2</sup> Karin M. Rabe, “Antiferroelectricity in oxides: A reexamination,” in *Functional Metal Oxides* (John Wiley and Sons, Ltd) Chap. 7, pp. 221–244.
- <sup>3</sup> Na Sai, B. Meyer, and David Vanderbilt, “Compositional inversion symmetry breaking in ferroelectric perovskites,” *Phys. Rev. Lett.* **84**, 5636–5639 (2000).
- <sup>4</sup> R. D. King-Smith and David Vanderbilt, “Theory of polarization of crystalline solids,” *Physical Review B* **47**, 1651–1654 (1993).
- <sup>5</sup> David Vanderbilt, *Berry Phases in Electronic Structure Theory: Electric Polarization, Orbital Magnetization and Topological Insulators* (Cambridge University Press, 2018) Chap. 3.
- <sup>6</sup> Yubo Zhang, Jianwei Sun, John P. Perdew, and Xifan Wu, “Comparative first-principles studies of prototypical ferroelectric materials by lda, gga, and scan meta-gga,” *Phys. Rev. B* **96**, 035143 (2017).
- <sup>7</sup> J. B. Neaton, C. Ederer, U. V. Waghmare, N. A. Spaldin, and K. M. Rabe, “First-principles study of spontaneous polarization in multiferroic BiFeO<sub>3</sub>,” *Phys. Rev. B* **71**, 014113 (2005).
- <sup>8</sup> Nicola A. Spaldin, “A beginner’s guide to the modern theory of polarization,” *Journal of Solid State Chemistry* **195**, 2–10 (2012).
- <sup>9</sup> Tess E. Smidt, Stephanie A. Mack, Sebastian E. Reyes-Lillo, Anubhav Jain, and Jeffrey B. Neaton, “An automatically curated first-principles database of ferroelectrics,” *Scientific Data* **7**, 72 (2020).
- <sup>10</sup> Raffaele Resta, “Macroscopic polarization in crystalline dielectrics: the geometric phase approach,” *Rev. Mod. Phys.* **66**, 899–915 (1994).
- <sup>11</sup> Takahiro Fukui, Yasuhiro Hatsugai, and Hiroshi Suzuki, “Chern numbers in discretized brillouin zone: Efficient method of computing (spin) hall conductances,” *Journal of the Physical Society of Japan* **74**, 1674–1677 (2005), <https://doi.org/10.1143/JPSJ.74.1674>.
- <sup>12</sup> Small rotations in going from *A* to *B* present no difficulty, since in practice the calculations are done in internal (i.e., lattice-vector) coordinates. For the same reason, a change in strain state presents no difficulties in principle, but can require some attention to the details of indexing of reciprocal lattice vectors.
- <sup>13</sup> John Bonini, “Berry flux diagonalization implementation,” <https://github.com/jrbp/berry-flux-diag>.
- <sup>14</sup> D. R. Hamann, “Optimized norm-conserving vanderbilt pseudopotentials,” *Phys. Rev. B* **88**, 085117 (2013).
- <sup>15</sup> Xavier Gonze, Bernard Amadon, Gabriel Antonius, Frdric Arnardi, Lucas Baguet, Jean-Michel Beuken, Jordan Bieder, Franois Bottin, Johann Bouchet, Eric Bousquet, Nils Brouwer, Fabien Bruneval, Guillaume Brunin, Tho Cavignac, Jean-Baptiste Charraud, Wei Chen, Michel Ct, Stefaan Cottenier, Jules Denier, Grgory Geneste, Philippe Ghosez, Matteo Giantomassi, Yannick Gillet, Olivier Gingras, Donald R. Hamann, Geoffroy Hautier, Xu He, Nicole Helbig, Natalie Holzwarth, Yongchao Jia, Franois Jollet, William Lafargue-Dit-Hauret, Kurt Lejaeghere, Miguel A.L. Marques, Alexandre Martin, Cyril Martins, Henrique P.C. Miranda, Francesco Naccarato, Kristin Persson, Guido Petretto, Valentin Planes, Yann Pouillon, Sergei Prokhorenko, Fabio Ricci, Gian-Marco Rignanesi, Aldo H. Romero, Michael Marcus Schmitt, Marc Torrent, Michiel J. van Setten, Benoit Van Troeye, Matthieu J. Verstraete, Gilles Zrah, and Josef W. Zwanziger, “The abinitproject: Impact, environment and recent developments,” *Computer Physics Communications* , 107042 (2019).
- <sup>16</sup> Shyue Ping Ong, William Davidson Richards, Anubhav Jain, Geoffroy Hautier, Michael Kocher, Shreyas Cholia, Dan Gunter, Vincent L. Chevrier, Kristin A. Persson, and Gerbrand Ceder, “Python materials genomics (pymatgen): A robust, open-source python library for materials analysis,” *Computational Materials Science* **68**, 314 – 319 (2013).
- <sup>17</sup> Yoshitaka Uratani, Tatsuya Shishidou, Fumiyuki Ishii, and Tamio Oguchi, “First-principles predictions of giant electric polarization,” *Japanese Journal of Applied Physics* **44**, 7130–7133 (2005).
- <sup>18</sup> D.-W. Fu, H.-L. Cai, Y. Liu, Q. Ye, W. Zhang, Y. Zhang, X.-Y. Chen, G. Giovannetti, M. Capone, J. Li, and R.-G. Xiong, “Diisopropylammonium bromide is a high-temperature molecular ferroelectric crystal,” *Science* **339**, 425–428 (2013).
- <sup>19</sup> E.I. Blount, “Formalisms of band theory,” (Academic Press, 1962) pp. 305 – 373.
- <sup>20</sup> Nicola Marzari and David Vanderbilt, “Maximally localized generalized wannier functions for composite energy bands,” *Phys. Rev. B* **56**, 12847–12865 (1997).